Revision 3

Wordcount: 6008

Halogen (F, Cl, Br, I) contents in silt and clay fractions of a Cambisol from a temperate forest

Tatjana Epp[1,2]*, Michael A.W. Marks[1], Harald Neidhardt[2], Yvonne Oelmann[2], Gregor Markl[1]

[1] Geoscience, University of Tübingen, Schnarrenbergstraße 94-96, 72076 Tübingen, Germany; tatjanaepp@web.de, michael.marks@uni-tuebingen.de, markl@uni-tuebingen.de

[2] Geoecology, University of Tübingen, Rümelinstraße 19-23, 72070 Tübingen, Germany; harald.neidhardt@uni-tuebingen.de, yvonne.oelmann@uni-tuebingen.de

*Corresponding author: Tatjana Epp, tatjana.epp@uni-tuebingen.de

Abstract

In spite of considerable efforts to understand the role of halogens (F, Cl, Br, I) in soil, concentration data for different soil size fractions is still sparse and information on the sorption behavior of halogens in natural soils is limited. We determined total halogen concentrations in different soil horizons and particle size fractions (i.e., coarse silt with 20-63 µm, medium and fine silt with 2-20 µm, coarse clay with 0.2- < 2 µm and medium clay with 0.02-0.2 µm) of a Cambisol from a temperate forest ecosystem in SW Germany. Further, we estimated the minimum proportions of sorbed halogens onto clay minerals and pedogenic oxides for different soil horizons and different particle size fractions.

Vertical depth profiles of halogens in the individual soil particle size fractions matched with the bulk soil vertical patterns. The lack of vertical differences of total halogens concentrations (F_{tot}, Br_{tot} and I_{tot}) in the mineral soil during soil development may be due to steady state or equilibrium conditions between weathering, sorption processes and surface input. In contrast, the vertical depth pattern of Cl_{tot} tended to decrease, suggesting the process of Cl accumulation in the topsoil and nutrient uplift. While F was likely mainly incorporated into the crystal lattice of clay minerals and gibbsite occupying OH-sites, significant amounts of the halogens with larger ionic radii (Cl, Br and I) were sorbed. The largest amounts (around 90% Cl and 70% Br and I, respectively) were sorbed on the smallest particle size fraction investigated (medium clay fraction; 0.02-0.2 μm), although this fraction only contributed about 1 wt% to the bulk soil. This is probably related to the highest sorption capacity of small particles due to their large surface area.

Our study provides new data on sorption behavior of the various halogens in soils of forest ecosystems which is different between F and the heavier halogens (Cl, Br, I) and further depends on soil particle sizes. The understanding of the chemical behavior of halogens in soils has implications for retention processes of pollutants in landfills or radioactive waste disposal.

Key words: Sorption processes, particle size fractions, Cambisol, fluorine, chlorine bromine, iodine

Introduction

The halogens, fluorine (F), chlorine (Cl), bromine (Br) and iodine (I) are important elements in natural ecosystems and their understanding is necessary for a variety of organic and inorganic reactions in soils, the critical zone and in the Earth's crust in general (e.e., Fuge 1988; Bastviken et al. 2007; Redon et al. 2011; Öberg and Bastviken 2012; Kendrick and Burnard 2013). While

Cl is an essential micro-nutrient for plants and micro-organisms (Raven 2017), F, Br and I are no essential micro-nutrients but appear to be involved in a large variety of organic processes (e.g., Yuita 1983; Fuge 1988; Marschner 1995; Kabata-Pendias 2011), and act as important ligands in inorganic processes like metal transport (Lecumberri-Sanchez and Bodnar 2018). In large concentrations halogens can have harmful effects on living organisms (Chubar et al. 2005). Processes within soils (such as halogenation; e.g., Asplund and Grimvall 1991; Montelius et al. 2015; Montelius et al. 2016) and external halogen input (such as atmospheric deposition, wash-off, and canopy leaching; e.g., Lovett et al. 2005; Roulier et al. 2019) strongly influence the halogen distribution in soils. The Cl distribution, for example, is strongly governed by chlorination processes in the organic layer which result in an accumulation of Cl_{tot} ($_{tot}$ = organic + inorganic fractions) in the organic layer and decreasing Cl_{tot} concentrations with increasing soil depth (e.g., Bastviken et al. 2007; Montelius et al. 2016; Epp et al. 2020). In contrast, F_{tot}, Br_{tot} and I_{tot} concentrations increase with increasing soil depth (Epp et al. 2020), which may be linked to sorption on for example positively charged surfaces of pedogenic oxides (iron (Fe), manganese (Mn) and aluminum (Al) oxides and (oxy) hydroxides) that form during pedogenesis (Gerzabek et al. 1999; Loganathan et al. 2007; Cortizas et al. 2016; Roulier et al. 2019). Further explanations for these depth profiles could be weathering and subsequent leaching (Davison and Weinstein 2006; Liu et al. 2014 and references therein; Fuge 2019) or the combination of the level of for example bromination linked to the age of SOM and stabilization of brominated organic substances by complexation with Al (Cortizas et al. 2016).

Modification of host rock material and primary mineral weathering and formation of secondary minerals such as clay minerals are governed by progressive soil formation (Chadwick and Chorover 2001; Cornelis et al. 2014). In general, soils consist of highly variable particle size mixtures with gaseous and liquid interstitial phases. Numerous reactions such as sorption and desorption processes take place at interfaces of water and charged surfaces of the solid soil

71 phase, for instance clay minerals or pedogenic oxides (Scheffer et al. 1998; Schoonheydt and
72 Johnston 2006). These sorption processes are strongly dependent on the size and type of the
73 particle surfaces, where the specific surface size increases with decreasing particle size. With
74 respect to silicate phases, allophane (Al_2O_3*$(SiO_2)_{1.7}$*$(H_2O)_{2.8}$) and imogolite ($Al_2SiO_3(OH)_4$)
75 have the largest specific surfaces ranging between 700 and 1100 m^2 g^{-1} (Parfitt 1989; Scheffer
76 et al. 1998 and references therein). With specific surfaces between 600 and 800 mg^2 g^{-1} smectite
77 and vermiculite have the largest specific surfaces among clay minerals. In comparison, specific
78 surface areas of pedogenic oxides, like goethite and hematite range between 50 and 150 m^2 g^{-1},
79 whereas ferrihydrite has by far the largest surface of 300 to 400 m^2 g^{-1} (Parfitt 1989; Scheffer
80 et al. 1998 and references therein).

81 Due to their large specific surface area, clay minerals and pedogenic oxides are particularly
82 effective sorbents for a large variety of ions. While clay minerals are generally negatively
83 charged in the pH range of most soils, pedogenic oxides are rather positively charged and, thus,
84 can sorb anions (Scheffer et al. 1998) such as inorganic F^-, Cl^-, Br^- or I^-. Sorption of halogens
85 on pedogenic oxides or clay minerals increases with decreasing pH (Weerasooriya and
86 Wickramarathna 1999; Goldberg and Kabengi 2010). Decreasing sorption behavior is linked to
87 increasing solution ionic strength of the background electrolyte and no adsorption was reported
88 at pH 8.8, the point of zero net proton charge (Weerasooriya and Wickramarathna 1999). With
89 regard to sorption of ions, two scenarios are distinguished: (1) inner-sphere adsorption, where
90 ligand exchange takes place, hence the ion and the ligands which form complexes are in direct
91 contact, and (2) outer-sphere adsorption, where hydrated ions are bound to mineral surfaces by
92 electrostatic interactions, i.e., where water molecules are interconnected between ions and the
93 ligands (e.g., Sposito 1989; Scheffer et al. 1998; Strawn and Sparks 1999). Fluoride was
94 described to form inner-sphere complexes with pedogenic oxides, while Cl^-, Br^- and I^- have
95 been found to show relatively weak adsorption behavior on clay minerals and oxides and are

96 suggested to rather form outer-sphere complexes (Scheffer et al. 1998; Eskandarpour et al.
97 2008; Li et al. 1995; Goldberg and Kabengi 2010; Petkovic et al. 1994; Chubar et al. 2005;
98 Weerasooriya and Wickramarathna 1999; Kaplan et al. 2000).

99 The objective of this study was to assess the total (sum of organic + inorganic) halogen
100 concentrations (F, Cl, Br, I) of three soil horizons in four particle size fractions (i.e., 20-63 µm
101 (coarse silt), 2-20 µm (fine and medium silt), 0.2 - < 2 µm (coarse clay) and 0.02 – 0.2 µm
102 (medium clay) in the mineral soil of a Cambisol. We further estimated minimum proportions
103 of sorbed halogens onto clay minerals and pedogenic oxides and investigated differences in the
104 sorption behavior of F and Cl, Br and I. Furthermore, we paid attention to potential vertical
105 depth patterns of total halogen concentrations. The distinction between organic and inorganic
106 halogens was not addressed in the present study.

107 ## Material and Methods

108 ### Study area

109 We investigated a Cambisol developed on gneissic host rock located in a spruce forest (*Picea*
110 *abies* (L.) H. Karst). Typically, this soil type consists of an organic layer on top of the mineral
111 soil, a mineral topsoil and mineral subsoil (Fig. 1). The investigated soil samples derive from
112 the Kammentobel valley, close to the Feldberg peak in the Schwarzwald, SW Germany (Tab.
113 1). The annual temperature in 2018 ranged between 23 and -20 °C and total precipitation was
114 ~1500 mm (Deutscher-Wetterdienst 2019; WetterKontor 2019). The samples of this study
115 represent a carefully selected subset of soil samples that were previously analyzed by Epp et al.
116 (2020) regarding their bulk halogen (F, Cl, Br and I) composition and pedogenic oxide content
117 (see chapter 2.3). The vegetation comprises spruce trees (*Picea abies* (L.) H. Karst) and
118 blueberry (*Vaccinium myrtillus* L.). The investigated soil can be classified as Cambisol
119 according to IUSS-Working-Group-WRB (2015) and developed on strongly weathered
120 gneisses (migmatites) from the Schwarzwald low mountain range. The investigated soil profile

121 comprises a depth of 57 cm and soil horizon Bw2C in the subsoil can be found until a depth of
122 ~ 70cm, then the transition to the host rock is reached. In total, triplicate samples from each soil
123 horizon i.e., mineral topsoil (Ah) and subsoil (Bw1, Bw2C) were selected. Further details on
124 the study site are given in Epp et al. (2020). The vertical halogen distribution in the four
125 investigated particle sizes will be presented as a preliminary data set and is included in this
126 study as there have not been many studies on this topic so far.

127 Sample preparation

128 The soil material used in this study was first sieved (< 2 mm) and dried at 40 °C for five days
129 in order to minimize loss of halogens to the gaseous phase. For further investigation, respective
130 samples from each location were combined to form composite samples. The dry and sieved soil
131 samples (< 2 mm) were then mixed with Millipore water (18.2 MΩ*cm). Subsequently the soil
132 water mixture was passed through 500, 250, 125, 63 and 20 µm stainless steel sieves to capture
133 the remaining solid material after each sieve size for further size-specific particle separation.

134 The fraction < 20 µm was transferred into a 1 L Atterberg cylinder with a drop height of 25 cm
135 and suspended with Millipore water. This procedure was applied to separate the clay fractions
136 < 2 µm from the remaining medium and fine silt fraction (2-20µm) according to Stokes' law
137 (Stokes 1901) as described by Atterberg (1912). Note that the clay particle size fractions do,
138 from a mineralogical point of view, not exclusively consist of clay minerals, but also contain to
139 a certain extent pedogenic oxides. The sediment was shaken in the cylinder and left to stand for
140 22 hours. During this period heavier silt and sand sized particles (> 2 µm) sedimented, whereas
141 clay-sized particles (< 2 µm) remained in suspension and could be separated from the
142 remainder. Subsequently, the cylinder was refilled with Millipore water and the procedure was
143 repeated until the supernatant liquid was no longer muddy. Depending on the soil horizon, this
144 procedure took up to 10 runs for the mineral top- and subsoil.

The obtained clay fractions < 2 µm were then separated by vacuum filtration (Welch Ilmvac^{TM}) using 0.8 µm cellulose nitrate membrane filters with a diameter of 10 cm (neoLab®). In order to separate the coarse clay (0.2- < 2 µm) from the medium clay (0.02-0.2 µm) fraction, all samples were cooled-centrifuged with a ROTANTA 460RS, using a 5624 rotor. The separation was conducted according to Tributh and Lagaly (1986) and the following frame conditions were applied: 100 ml plastic centrifuge tubes with a diameter of 4 cm, r_0 = 10.3 cm, r = 12.3 cm and the sediment was mixed with 80 ml Millipore water. As a first step, the fine clay fraction (< 0.02 µm) was separated by 4400 rotations per minute (RPM min^{-1}) for t = 6 h 22 min. Subsequently, the first 2 cm were sampled by pipetting and the tubes were refilled with Millipore water to 80 ml. In total, three runs were implemented, but it turned out that the fine clay fraction) was too fine to get reliably completely separated or used for further investigations. Since the fine clay fraction was partly removed and not further considered, it is only referred to the medium clay fraction as the finest fraction. In order to separate the medium clay fraction from the coarse clay fraction, the samples were centrifuged at 2000 RPM min^{-1} for t = 21 min. In total 57 runs were required to separate the fine and medium from the coarse clay fraction.

In order to minimize potential contamination with halogens we did not use H_2O_2 to eliminate organic particles or any dispersing agents (such as HCl) as pre-treatment in any of the separation steps. Therefore, the determined halogen concentrations of the samples represent the sum of organic and inorganic halogen components. By using Millipore water during sieving and grain size separation steps, water-soluble (and loosely bound/exchangeable) halogens were removed prior the analyses. We know from previous analysis that in the bulk soil, water-extractable halogen proportions ranged from 0.4 % (F) to 9 % (Cl) (Epp et al. (2020). Note that total halogen concentrations (F_{tot}, Cl_{tot}, Br_{tot}, I_{tot}; i.e., organic + inorganic halogens) of all three soil horizons (Ah, Bw1, Bw2C) based on combustion ion chromatography (CIC, see halogen

169 analyses below) measurements represent both halogens incorporated in the crystal lattice and
170 halogens sorbed to particle surfaces.

171 Possible organic contamination during sample treatment can be excluded, since total organic
172 carbon (C_{org}) content of soil fractions was 40 % lower than total C_{org} of bulk soil. The different
173 particle size fractions contained various C_{org} amounts. The bulk C_{org} concentration in soil
174 horizon Bw1 (after taking the relative amount compared to bulk soil into consideration)
175 contained in the coarse silt fraction 6 g kg^{-1}, in the medium and fine silt fraction 10 g kg^{-1}, in
176 the coarse clay fraction 1 g kg^{-1} and in the medium clay fraction < 1 g kg^{-1}.

177 Desorption experiments

178 To remove strongly sorbed halogens on soil particles, the already grain size-separated samples
179 were mixed with a solution of 350 mg K_2HPO_4 (≥ 99%, Roth) in 10 mL Millipore water for
180 which the pH was adjusted to 3-4 by adding 140 µL HNO_3 (65 %, suprapure, Merck). It is
181 generally known that phosphate is highly exchangeable with other anions (Manning and
182 Goldberg 1996). Kaolinite and illite generally have a specific surface area of 10 - 100 m^2 g^{-1},
183 whereas clay minerals and pedogenic oxides in extreme cases reach values up to 1000 m^2 g^{-1}
184 (Parfitt 1989; Santamarina et al. 2002 and references therein). These values are most likely only
185 representative of the smaller grain size fractions and thus represent maximum specific surface
186 areas. To assure excess of phosphate, we assumed a total specific surface area of 1000 m^2 g^{-1}
187 and used an initial phosphate content of 2.5 µmol m^{-2} (Torrent et al. 1990). Each analyzed
188 sample varied with respect to total mass used and the total surface area of our samples reached
189 up to 150 m^2. For this maximum surface 0.4 mmol would have sufficed, thus we have used a 2
190 mmol phosphate to provide more than adequate surface coverage. The samples were left in the
191 solution for three days and were occasionally shaken. The silt fractions were then separated
192 from the K_2HPO_4 solution by vacuum filtration, briefly washed with Millipore water and
193 subsequently dried at room temperature. The clay fractions were centrifuged and supernatant

194 solutions pipetted. The same procedure was repeated with Millipore water as a wash step and
195 solid samples were dried at room temperature for subsequent analysis by CIC.

196 Halogen analyses

197 After size fractionation, all samples were manually mortared and homogenized before analysis
198 of total halogen concentrations by combustion ion chromatography (CIC). The same applies to
199 subsamples that have been additionally treated with K_2HPO_4 to remove the surface-sorbed
200 halogens and to solely assess the residual fraction of mostly structurally bound halogens. For
201 the CIC analyses, an autosampler for solid samples (MMS 5000; Analytik Jena) connected to a
202 combustion oven and to a 930 Compact IC Flex chromatograph (Metrohm, Germany) with
203 chemical suppression and a peristaltic pump for regeneration (100 mmol L^{-1} H_2SO_4) was used.
204 In brief, inorganic and organic halogens in a sample are transformed into inorganic forms and
205 are transferred into the gaseous phase through combustion. The halogens are trapped from the
206 carrier gas by an adsorption solution that is transferred to an IC column. Separation of analytes
207 was achieved with a Metrosep A Supp 5 – 250/4.0 column (Metrohm) using an eluent consisting
208 of 8 mmol L^{-1} Na_2CO_3 (suprapure, Merck ®). The limits of detection were: 0.8 mg kg^{-1} for F,
209 0.2 mg kg^{-1} for Cl and 0.02 mg kg^{-1} for Br and I (calculated according to DIN 32645). Based
210 on the analysis of standard solutions (single element solutions of F, Cl, Br and I; Roth; 1000
211 mg L^{-1}) and various reference materials (SO3, GSN), the long-term reproducibility (1σ) was
212 within a 20 % margin for F and 10 % for Cl, Br and I. A detailed description of the analytical
213 method can be found in Epp et al. (2019).

214 Liquid samples of the residual K_2HPO_4 extraction solution were analyzed for F_{inorg} and Cl_{inorg}
215 using an autosampler for liquid samples (858 Professional Sample Processor, Metrohm). The
216 extraction solutions were filtered in the ion chromatograph, which contains an internal filter of
217 0.2 μm pore size. Limits of detection were for F 0.2 mg L^{-1} and for Cl 0.5 mg L^{-1} (calculated

218 according to DIN 32645), while Br_{inorg} and I_{inorg} concentrations were below the detection limit
219 as the samples have been diluted by a factor of 1000 to avoid column overload by phosphate.
220
221 Complementary analyses

222 We used dried (40 °C) and sieved (<2 mm) bulk sample material for the analyses of pedogenic
223 oxides. The analyses of poorly crystalline pedogenic oxides (Fe_{ox} and Al_{ox}) and the sum of
224 poorly crystalline and crystalline pedogenic oxides (Fe_d and Al_d) have already been reported in
225 Epp et al. (2020). Hence, further methodical aspects can be found in this previous study. Coarse
226 clay and medium clay fractions of soil horizons Ah, Bw1 and Bw2C were analyzed by means
227 of X-ray diffraction (XRD). The XRD analyses were conducted on texture samples on a glass
228 slide with preferred orientation using a Bruker D8 Advance at the University of Tübingen. Total
229 carbon (C_{tot}) concentrations were analyzed from homogenized samples with an Elemental
230 Analyzer (Vario EL III, Elementar Analysensystem GmbH). Due to very minor amounts of
231 $CaCO_3$ (< 1 %) in the acidic mineral soil (pH < 4.5), C_{tot} is considered to be adequate to total
232 organic C (C_{org}).

233 Data analysis

234 IBM® SPSS® Statistics Version 25 was used for all statistical evaluation. Spearman rank
235 correlations were conducted to detect possible correlations between halogen concentrations and
236 various soil parameters. Generally, for $p < 0.05$, differences and correlations were considered
237 as statistically significant. The Shapiro-Wilk test was applied to test for normal distribution and
238 the Levene test was assessed for checking the homogeneity of variances. If homogeneity of
239 variance was not given, the Welch test was used and the Games-Howell as post-hoc test.
240 Halogen concentrations of F_{sorb}, Cl_{sorb}, Br_{sorb} and I_{sorb} between different particle sizes were
241 compared using the one-way ANOVA to determine possible relations of halogen concentrations
242 and grain size.

243

244 # Results

245 ## Soil properties

246 On average, 40 wt% of bulk soil consisted of coarse silt (20-63 µm; 15 wt%) and fine to medium
247 silt (2-20 µm; 25 wt%) particles. The clay fractions represented by far the smallest weight
248 portion of the investigated bulk soil, with 3 wt% of coarse clay (0.2- < 2 µm) and <1 wt% of
249 medium clay (0.02- 0.2 µm) particles, only. Based on XRD analyses, coarse and medium clay
250 samples were composed of vermiculite, illite, kaolinite and gibbsite, i.e., did not contain any
251 swellable clay minerals. The organic carbon concentration in the different particle size fractions
252 ranged between 2.5 and 10 wt. % (Tab. 2) and was on average about 15 % lower after phosphate
253 treatment (Fig. 2a). In the following, we present first total halogen concentrations (X_{tot}) in the
254 samples, followed by a summary of the results of the desorption experiments.

255 ## Total halogen concentrations

256 Total F concentrations of all four particle size fractions overlapped across the vertical depth
257 profile, the concentrations ranging between 500 and 1200 mg kg^{-1}. Within the mineral soil, F_{tot}
258 concentrations were relatively constant (Fig. 3) and overall, F_{tot} concentrations were negatively
259 correlated with the particle size (r = -0.536, p = 0.002).

260 Total Cl concentrations in the vertical profile tended to show a slight decrease in all four particle
261 sizes with increasing soil depth (Fig. 3). In the coarse silt, medium and fine silt and in the coarse
262 clay fractions Cl_{tot} concentrations ranged between 100 and 180 mg kg^{-1}, but very high Cl_{tot}
263 concentrations occurred in the medium clay fraction with up to 2500 mg kg^{-1} Cl (Fig. 3). In
264 addition, Cl_{tot} concentrations were negatively correlated with particle size (r = -0.405, p =
265 0.021).

Vertical Br_{tot} concentration profiles showed a tendency to increase with depth in all four particle sizes (Fig. 3) and with decreasing particle size Br_{tot} concentrations increase (r = -0.863, p < 0.001). This is indicated by vertical profiles that tend to be shifted to higher concentrations with decreasing particle size instead of overall overlapping profiles. Similar to what was observed with Cl_{tot}, Br_{tot} concentrations were highest in the medium clay fraction (140 to 220 mg kg^{-1}), somewhat higher than in the coarse silt, medium and fine silt fraction and in the coarse clay fraction (20 and 80 mg kg^{-1}).

Similarly, I_{tot} concentrations tended to increase with depth in all four particle sizes (Fig. 3) and were negatively correlated with particle size (r = -0.820, p < 0.001). The concentrations increased with decreasing particle size, since the vertical profiles did hardly overlap but instead tended to shift to higher concentrations with decreasing particle size. Total I concentrations ranged in the coarse silt, the medium and fine silt fraction and in the coarse clay fraction from 6 to 26 mg kg^{-1} and in the medium clay fraction from 25 to 60 mg kg^{-1}.

In almost all samples, F_{tot} concentrations were by far higher than Cl_{tot}, Br_{tot} and I_{tot} and only for the smallest grain size fraction (medium clay), Cl_{tot} was similar to F_{tot}. (Tab. 2). Molar halogen ratios were similar in the coarse silt fraction (F/Cl = 8, F/Br = 70, F/I =390), in the medium and fine silt fraction (F/Cl = 10, F/Br = 50, F/I = 200), and in the coarse clay fraction (F/Cl = 10, F/Br = 45, F/I = 250), while in the medium clay fraction, F/Cl = 1, F/Br = 15 and F/I = 100. Concentration differences among Cl, Br and I were not large, as the molar ratio of Cl/Br was on average 8 (and 50 for Cl/I), almost six times lower compared to the molar F ratios.

Sorption behavior

The difference between X_{tot} and remaining halogens in the solid phase after phosphate treatment was interpreted as strongly sorbed halogens (X_{sorb}). The remaining halogens in the samples largely represent halogens that are incorporated into crystal lattices (X_{inc}) and potentially unknown amounts of soil-bound organo-halogens. These cannot be quantified by our method,

as phosphate treatment may not be sufficient to desorb such organically bound halogens. Thus, the calculated amounts of sorbed halogens represent minimum values. Halogens in supernatant phosphate solutions represent the dissolved inorganic concentrations (X_{inorg}). Notable differences between F and Cl, Br and I with regard to sorbed proportions are as follows:

Fluorine

In almost all size fractions, F was mostly structurally bound (i.e., incorporated into crystal latices) and only small amounts of the total F (generally <10 %) where sorbed (Tab. 2, Fig. 4) that did not differ significantly between the particle sizes ($p > 0.05$). Only in the 20-63µm fraction of soil horizon Bw1 around 50 % of F were sorbed (Tab. 2, Fig. 4). Dissolved F_{inorg} concentrations in the supernatant phosphate solution were generally decreasing with soil depth (Fig. A1).

Chlorine

In the coarse, medium and fine silt fractions, Cl_{inc} concentrations tended to decrease with depth from 150 to 90 mg kg^{-1} (Tab. 2), with on average 20 % Cl_{sorb} (Fig. 4). In the coarse clay fraction Cl_{inc} tended to decrease slightly with depth (130 to 110 mg kg^{-1}; Tab. 2), with 25-30 % Cl_{sorb} in soil horizons Ah and Bw2C, but only 5 % Cl_{sorb} in Bw1 (Fig. 4). In contrast, in the medium clay fraction, most Cl (>80 %) is sorbed (Tab. 2). Dissolved Cl_{inorg} in the supernatant phosphate solutions varied between 0.4 and 4.5 mg L^{-1} irrespective of soil depth (Fig. A1).

Bromine

In the coarse silt fraction, Br_{inc} concentrations tended to decrease with depth from 40 to 25 mg kg^{-1} and on average, only 10% of Br_{tot} were sorbed (Tab. 2, Fig. 4). In the medium and fine silt fraction Br_{tot} concentrations tended to increase with depth from 40 to 70 mg kg^{-1}. In soil horizon Ah only 3 % sorbed, whereas in the mineral subsoil 30 % was sorbed (Tab. 2, Fig. 4). In the

coarse clay fraction, on average 20 % Br was sorbed and the highest portion of Br (60-70%) was sorbed in the medium clay fractions, similar to what was observed for Cl (Tab. 2, Fig. 4).

Iodine

In the coarse silt fraction I_{inc} concentrations tended to decrease with depth from 7 to 2 mg kg^{-1} (Tab. 2). Only about of 5 % of I_{tot} was sorbed in the Ah horizon, whereas it was between 60 and 70 % in soil horizons Bw1 and Bw2C (Fig. 4). In the medium and fine silt fractions I_{inc} concentrations varied between 5 and 9 mg kg^{-1} with on average 60 % of $I_{sorb.}$ Similar observations were made in the coarse clay and medium clay fractions (8 - 13 mg kg^{-1} and 12 – 18 mg kg^{-1} I_{inc}, respectively) with 50 -70 % of I_{sorb}.

Discussion

Total halogen concentrations in different soil size fractions

The patterns for F_{tot}, Cl_{tot}, Br_{tot} and I_{tot} in soil size fractions < 63 µm (this study), were very similar to those of bulk soil sample profiles described in Epp et al. (2020), which included particle sizes up to 2 mm (Fig. 3). Bulk soil data was always in the lower concentration range compared to halogen concentrations analyzed in the present study (Fig. 3). This is explained by negligible amounts of clay minerals (Hosking et al. 1957) or pedogenic oxides in soil size fractions > 63 µm, resulting in lower total halogen concentrations.

F_{tot} profiles of all investigated soil size fractions did not show any vertical patterns with depth (Fig. 3). All vertical F_{tot} profiles strongly overlapped, thus no concentration differences emerged between the individual soil fractions (Fig. 3).

High F concentrations in soil are due to weathering of F-rich minerals in the host rock (Totsche et al. 2000; Zhang et al. 2010 and references therein). The host rock of the study site contains

337 F-bearing minerals such as biotite, and F released by weathering can subsequently be
338 incorporated into secondary clay minerals or adsorbed onto pedogenic oxides. Commonly, the
339 intensity of weathering in a vertical soil profile decreases with increasing depth (Linser and
340 Scharrer 1966) and thus, it is expected that F, pedogenic oxide or clay mineral concentrations
341 should show distinctive depth patterns. However, concentrations of pedogenic oxides and clay
342 minerals did not vary within the top- and subsoil (Fig. 2 c & d) and point to a constant intensity
343 of weathering in the depth profile. Very low Fe_{ox}/Fe_d ratios between 0.06 and 0.1 of the soil
344 column (Epp et al. 2020) indicated that scarcely any iron from silicate weathering is supplied.
345 Formerly present biotite from the host rock may already be entirely dissolved. Hence, no
346 vertical concentration differences of F_{tot} within the mineral soil may be attributed to steady state
347 or equilibrium conditions between F-release by weathering, subsequent surface adsorption or
348 incorporation into the crystal lattice of clay minerals and gibbsite and surface input and
349 subsequent accumulation in upper soil horizons. Besides, the lack of differences between the
350 soil horizons during soil development could have been caused by a low solubility and slow
351 reaction kinetics of clay minerals (Meyer and Howard 1983).

352 Within the top- and subsoil, Cl_{tot} was also relatively constant. Since the organic particles were
353 not explicitly removed during sample preparation, it is very likely that the investigated samples
354 still contained organic compounds which either incorporated or adsorbed halogens. The
355 tendency for vertical depth patterns of Cl point to an accumulation of Cl in the Ah horizon and
356 probably nutrient uplift in the subsoil, hence, the same processes as in the bulk soil (see details
357 in Epp et al. 2020). Chlorination in the organic layer is the underlying fixation process which
358 results in an accumulation of Cl in the organic layer and in the Ah horizon (Hjelm et al. 1995
359 and references therein; Öberg and Grøn 1998; Redon et al. 2011). The lack of depth variations
360 may indicate steady state or equilibrium conditions between surface input, sorption processes

and nutrient uplift. Also large reservoirs of Cl in soil (e.g., Redon et al. 2011) could have led to the lack of differences in the horizons during soil development.

With regard to sorption processes, higher adsorption to soil particles in subsoil horizons (deeper than 50 cm) was described by Li et al. (1995) for the case of Br and was attributed to exchange reactions between Br and negatively charged organic compounds. The same study reported adsorption of Br to be rather negligible in the topsoil (upper 50 cm). These results are in contrast to our findings, since sorption of Br in the topsoil was not negligible, and we found on average a minimum amount of 11 % of Br_{tot} to be sorbed to pedogenic oxides or organic compounds. Such contrasting findings can be explained by different soil types and concomitant soil properties. In the study of Li et al. (1995) a Spodosol was investigated which is typically characterized by a low pH, moist and acidic conditions which results in redistribution of organic matter and Fe- and Al oxides from mineral topsoil into the mineral subsoil (Yli-Halla et al. 2006; Chesworth et al. 2008). In contrast, our investigated Cambisol showed organic soil horizons (Oi and Oe) on top and in the different particle size fractions a C_{org} concentration of up to 10 % in the mineral top- and subsoil (Ah, Bw1 and Bw2C) clearly indicating the presence and the potential importance of organic compounds. The discrepancy with our data can be explained by different soil properties. The Bw1 soil horizon in our investigated Cambisol contains pedogenic oxides where Br_{inorg} sorption is significant, also in depths > 50 cm.

Although the medium clay fraction only contributes 1 wt% to bulk soil, F_{tot} concentrations in this fraction were the same as in the other investigated fractions. In addition, around 50 wt% of Br_{tot} and I_{tot} and even 70 wt% of Cl_{tot} were found in the medium clay fraction. Similar or even much higher concentrations in samples that contribute only marginally to the total sample weight further indicate the importance of halogen incorporation and sorption processes in soils. In sum, our results showed that the lack of halogen variations with depth may be due to

equilibrium conditions between weathering, sorption processes and surface input. Besides, large halogen pools may inhibit vertical concentration differences during soil development.

Differences in sorption behavior between F and the heavier halogens (Cl, Br, I)

Fluorine has a much smaller radius compared to Cl, Br and I (Latscha et al. 2011). Also, changes in ionic strength have a very minor effect on the adsorption of F to kaolinite but strongly affects Cl, Br and I adsorption, which has been interpreted to resemble inner-sphere complexation for F but outer-sphere complexation for Cl, Br and I (Weerasooriya and Wickramarathna 1999). Thus, we assume that compared to Cl, Br and I, F is less prone to be sorbed to surfaces but is rather incorporated into the crystal lattice of, for example, clay minerals (e.g., kaolinite, illite) and gibbsite, occupying OH-sites (Romo 1054; Kau et al. 1998; Weerasooriya et al. 1998; Bower and Hatcher 1967). The substitution of OH^- by F^- in clay minerals is strongly pH-dependent (Romo and Roy 1957; Fuge 1988; Du et al. 2011) and is enhanced in acidic solutions (Chubar et al. 2005). The soil pH of 3-4 for the present location (Epp et al. 2020; Fig. 2b) offers therefore perfect conditions for an extensive OH^- exchange by F^-.

In contrast, anion substitution is not likely to be a valid mechanism for Cl^-, Br^- and I^-. Rather adsorption to mineral surfaces via outer-sphere complexation is expected for Cl, B^- and I (Weerasooriya and Wickramarathna 1999). In the pH range of common soils (including those of the investigated sample location, see above), pedogenic oxides mostly have positively charged surfaces (Scheffer et al. 1998 and references therein) and thus serve as sorbing agents for halogens. This was confirmed, for example, by positive correlations between total Br and total I concentrations and pedogenic oxides as already described in Epp et al. (2020).

Our results suggest that most F (on average 93 %) was incorporated into crystal lattices of minerals – likely of clay minerals, whereas on average and over all soil horizons, a least 32 % of Cl, 25 % of Br and 55 % of I were sorbed onto pedogenic oxides. On the other hand, this also means that significant amounts of Cl, Br and I have not been desorbed by phosphate

410 treatment (see subsection Sorption behavior of the Results section). This suggests that either
411 significant incorporation into the crystal lattice of clay minerals or pedogenic oxides happened,
412 or more likely, that soil-bound organo-halogens play a major role for the heavier halogens. To
413 investigate this further, alternative extractions (e.g., NaOH or TMAH) and surface-specific
414 analytical methods need to be applied.

415

416 ## Implications

417 The obtained data along with our previously published study allowed us to portray the sorption
418 behavior of F, Cl, Br and I in a vertical soil profile from a temperate forest in four different soil
419 size fractions. We found remarkable differences in the sorption behavior between F and the
420 other halogens (Cl, Br and I): For fluorine, total concentrations are relatively similar for all
421 particle sizes and the share of F_{sorb} is mostly low to negligible and largely independent from
422 particle size. In contrast, Cl_{tot}, Br_{tot} and I_{tot} concentrations increased with decreasing particle
423 size and were by far highest in the smallest soil fraction (0.02-0.2 μm) and further, about 90 %
424 of Cl_{tot} and about 70 % of Br_{tot} and I_{tot} are sorbed in the mineral subsoil (Fig. 4). In general,
425 sorption should increase with decreasing grain size (Sposito 1984; Scheffer et al. 1998), since
426 the specific surface size of particles is strongly dependent on the particle size (Sposito 1984).
427 Thus, our results for Cl, Br and I are in line with the generally expected halogen sorption
428 behavior.

429 Steady state or equilibrium conditions between weathering, sorption processes and surface
430 input probably caused lacking distinctive vertical concentration differences of F_{tot}, Cl_{tot}, Br_{tot}
431 and I_{tot} in the mineral soil during soil development. Other biogeochemical processes might be
432 negligible compared to the large halogen stocks in the soil which may inhibit visible
433 concentration differences. The fact that the medium clay fraction only accounted for 1 wt.% of

434 the bulk soil while it contained most of Cl, Br and I emphasized the importance of halogen
435 sorption to clay minerals and/ or pedogenic oxides.

436 Further understanding of sorption behavior on clay minerals may have implications for
437 retention of organic and inorganic pollutants. Landfill sludges can contain for example Cl-
438 bearing organic and inorganic pollutants. Material used in such landfills contain large amounts
439 of clay minerals which enhance the sorption of organic compounds. Furthermore, the
440 radionuclides ^{36}Cl and ^{129}I have a long half-life and their disposal and its effects are of current
441 importance. Thus, understanding the sorption behavior of halogens on for instance clay
442 minerals is crucial for retention processes of pollutants in landfills or potentially for radioactive
443 waste disposal. In conclusion, our results revealed the importance of sorption processes for Cl,
444 Br and I and incorporation processes for F which control the vertical halogen distribution in a
445 Cambisol of a temperate forest.

446 **Acknowledgements**

447 We are grateful to Frieder Lauxmann for his help with the XRD analyses. Further thank goes
448 to Lukas Schmid for his support with the centrifugation during the elaborate preparation
449 process. Annelie Papsdorf and Sabine Flaiz is thanked for the CN analyses. Furthermore, we
450 are very grateful to Christian Mikutta, Stefan Dultz and Peter Kühn for very constructive
451 discussions and to two anonymous reviewers for their insightful comments on an earlier version
452 of this manuscript. This study was funded by the German Research Foundation (DFG) [grant
453 numbers Ma2135/20-1, Oe516/8-1].

454

455 **References**

456 Asplund G, Grimvall A (1991) Organohalogens in nature. Environmental science & technology
457 25:1346-1350.

458 Atterberg A (1912) Die mechanische Bodenanalyse. Internationale Mitteilungen für
459 Bodenkunde:312-342.
460 Bastviken D, Thomsen F, Svensson T, Karlsson S, Sandén P, Shaw G, Matucha M, Öberg G
461 (2007) Chloride retention in forest soil by microbial uptake and by natural chlorination
462 of organic matter. Geochimica et Cosmochimica Acta 71:3182-3192.
463 Bower C, Hatcher J (1967) Adsorption of fluoride by soils and minerals. Soil Science 103:151-
464 154.
465 Chadwick OA, Chorover J (2001) The chemistry of pedogenic thresholds. Geoderma 100:321-
466 353.
467 Chesworth W, Camps Arbestain M, Macías F (2008) Calcareous Soils In Encyclopedia of Soil
468 Science; Chesworth, W., Ed. Springer: Dordrecht, Netherlands.
469 Chubar N, Samanidou V, Kouts V, Gallios G, Kanibolotsky V, Strelko V, Zhuravlev I (2005)
470 Adsorption of fluoride, chloride, bromide, and bromate ions on a novel ion exchanger.
471 Journal of colloid and interface science 291:67-74.
472 Cornelis J-T, Weis D, Lavkulich L, Vermeire M-L, Delvaux B, Barling J (2014) Silicon isotopes
473 record dissolution and re-precipitation of pedogenic clay minerals in a podzolic soil
474 chronosequence. Geoderma 235:19-29.
475 Cortizas AM, Vázquez CF, Kaal J, Biester H, Casais MC, Rodríguez TT, Lado LR (2016)
476 Bromine accumulation in acidic black colluvial soils. Geochimica et Cosmochimica Acta
477 174:143-155.
478 Davison AW, Weinstein LH (2006) Some problems relating to fluorides in the environment:
479 effects on plants and animals. Advances in Fluorine Science 1:251-298.
480 Deutscher-Wetterdienst (2019) Klimadaten Deutschland - Monats- und Tageswerte (Archiv).
481 Du J, Wu D, Xiao H, Li P (2011) Adsorption of fluoride on clay minerals and their mechanisms
482 using X-ray photoelectron spectroscopy. Frontiers of Environmental Science &
483 Engineering in China 5:212-226.
484 Epp T, Marks MA, Ludwig T, Kendrick MA, Eby N, Neidhardt H, Oelmann Y, Markl G (2019)
485 Crystallographic and fluid compositional effects on the halogen (Cl, F, Br, I)

incorporation in pyromorphite-group minerals. American Mineralogist 104:1673-1688. doi: https://doi.org/10.2138/am-2019-7068.

Epp T, Neidhardt H, Pagano N, Marks MA, Markl G, Oelmann Y (2020) Vegetation canopy effects on total and dissolved Cl, Br, F and I concentrations in soil and their fate along the hydrological flow path. Science of The Total Environment 712C:135473.

Eskandarpour A, Onyango MS, Ochieng A, Asai S (2008) Removal of fluoride ions from aqueous solution at low pH using schwertmannite. Journal of Hazardous Materials 152:571-579.

Fuge R (1988) Sources of halogens in the environment, influences on human and animal health. Environmental Geochemistry and Health 10:51-61. doi: 10.1007/bf01758592.

Fuge R (2019) Fluorine in the environment, a review of its sources and geochemistry. Applied geochemistry 100:393-406.

Gerzabek MH, Muramatsu Y, Strebl F, Yoshida S (1999) Iodine and bromine contents of some Austrian soils and relations to soil characteristics. Journal of plant nutrition and soil science 162:415-419.

Goldberg S, Kabengi NJ (2010) Bromide Adsorption by Reference Minerals and Soils. Vadose Zone Journal 9:780-786.

Hjelm O, Johansson M-B, Öberg-Asolund G (1995) Organically bound halogens in coniferous forest soil-Distribution pattern and evidence of in situ production. Chemosphere 30:2353-2364.

Hosking J, Neilson ME, Carthew A (1957) A study of clay mineralogy and particle size. Australian Journal of Agricultural Research 8:45-74.

IUSS-Working-Group-WRB (2015) World reference base for soil resources 2014- International soil classification system for naming soils and creating legends for soil maps. Food and Agriculture Organization of the United Nations, Italy, Rome, pp 203.

Kabata-Pendias A (2011) Trace elements in soils and plants. CRC Press.

Kaplan DI, Serne RJ, Parker KE, Kutnyakov IV (2000) Iodide sorption to subsurface sediments and illitic minerals. Environmental Science & Technology 34:399-405.

514 Kendrick MA, Burnard P (2013) Noble gases and halogens in fluid inclusions: A journey
515 through the Earth's crust The noble gases as geochemical tracers. Springer, pp 319-
516 369.
517 Kau P M H, Smith D W, Binning P (1998) Experimental sorption of fluoride by kaolinite and
518 bentonite. Geoderma 84: 89–108.
519 Latscha HP, Klein HA, Mutz M (2011) Allgemeine Chemie: Chemie-Basiswissen I. Springer-
520 Verlag.
521 Lecumberri-Sanchez P, Bodnar R (2018) Halogen Geochemistry of Ore Deposits:
522 Contributions Towards Understanding Sources and Processes In: Harlov DE,
523 Aranovich L (eds) The Role of Halogens in Terrestrial and Extraterrestrial Geochemical
524 Processes. Springer Geochemistry, pp 261-305.
525 Li Y, Alva A, Calvert D, Banks D (1995) Adsorption and transport of nitrate and bromide in a
526 spodosol. Soil science 160:400-404.
527 Linser H, Scharrer K (1966) Handbuch der Pflanzenernährung und Düngung. Springer-Verlag.
528 Liu X, Wang B, Zheng B (2014) Geochemical process of fluorine in soil. Chinese Journal of
529 Geochemistry 33:277-279.
530 Loganathan P, Liu Q, Hedley MJ, Gray CW (2007) Chemical fractionation of fluorine in soils
531 with a long-term phosphate fertiliser history. Soil Research 45:390-396. doi:
532 https://doi.org/10.1071/SR07030.
533 Lovett GM, Likens GE, Buso DC, Driscoll CT, Bailey SW (2005) The biogeochemistry of
534 chlorine at Hubbard Brook, New Hampshire, USA. Biogeochemistry 72:191-232. doi:
535 10.1007/s10533-004-0357-x.
536 Manning BA, Goldberg S (1996) Modeling competitive adsorption of arsenate with phosphate
537 and molybdate on oxide minerals. Soil Science Society of America Journal 60:121-131.
538 Marschner H (1995) Mineral nutrition of higher plants. 2nd. Edn Academic Pres.
539 Meyer D, Howard J (1983) Evaluation of clays and clay minerals for application to repository
540 sealing. D'Appolonia Consulting Engineers.

Montelius M, Thiry Y, Marang L, Ranger J, Cornelis J-T, Svensson T, Bastviken D (2015) Experimental evidence of large changes in terrestrial chlorine cycling following altered tree species composition. Environmental science & technology 49:4921-4928.

Montelius M, Svensson T, Lourino-Cabana B, Thiry Y, Bastviken D (2016) Chlorination and dechlorination rates in a forest soil—a combined modelling and experimental approach. Science of the total Environment 554:203-210.

Öberg G, Grøn C (1998) Sources of Organic Halogens in Spruce Forest Soil. Environmental Science & Technology 32:1573-1579. doi: 10.1021/es9708225.

Öberg G, Bastviken D (2012) Transformation of chloride to organic chlorine in terrestrial environments: variability, extent, and implications. Crit Rev Environ Sci Technol 42:2526-2545.

Parfitt R (1989) Phosphate reactions with natural allophane, ferrihydrite and goethite. Journal of Soil Science 40:359-369.

Petkovic MD, Milonjic SK, Dondur VT (1994) Determination of Surface Ionization and Complexation Constants at Colloidal Aluminum Oxide/Electrolyte Interface. Separation science and technology 29:627-638.

Redon P-O, Abdelouas A, Bastviken D, Cecchini S, Nicolas M, Thiry Y (2011) Chloride and Organic Chlorine in Forest Soils: Storage, Residence Times, And Influence of Ecological Conditions. Environmental Science & Technology 45:7202-7208. doi: 10.1021/es2011918.

Romo L A (1954) Role of lattice hydroxyls of kaolinite in phosphate fixation and their replacement by fluoride. Journal of Colloid Science 9: 385–392.

Romo L, Roy R (1957) Studies of the Substitution of OH–by F–in Various Hydroxylic Minerals. American Mineralogist: Journal of Earth and Planetary Materials 42:165-177.

Roulier M, Coppin F, Bueno M, Nicolas M, Thiry Y, Della Vedova C, Février L, Pannier F, Le Hécho I (2019) Iodine budget in forest soils: Influence of environmental conditions and soil physicochemical properties. Chemosphere.

568 Santamarina J, Klein K, Wang Y, Prencke E (2002) Specific surface: determination and
569 relevance. Canadian Geotechnical Journal 39:233-241.
570 Scheffer F, Schachtschabel P, Blume H, Hartge K, Schwertmann U, Brümmer G, Renger M
571 (1998) Lehrbuch der Bodenkunde/Scheffer/Schachtschabel. Ferdinand Enke Verlag,
572 Stuttgart.
573 Schoonheydt RA, Johnston CT (2006) Surface and interface chemistry of clay minerals
574 Developments in clay science. pp 87-113.
575 Sposito G (1984) The surface chemistry of soils. Oxford university press.
576 Sposito G (1989) The Chemistry of Soils. Oxford University Press, New York.
577 Stokes SGG (1901) Mathematical and physical papers. University Press, Cambridge.
578 Strawn DG, Sparks DL (1999) The use of XAFS to distinguish between inner-and outer-sphere
579 lead adsorption complexes on montmorillonite. Journal of Colloid and Interface Science
580 216:257-269.
581 Torrent J, Barron V, Schwertmann U (1990) Phosphate adsorption and desorption by goethites
582 differing in crystal morphology. Soil Science Society of America Journal 54:1007-1012.
583 Totsche KU, Wilcke W, Körber M, Kobza J, Zech W (2000) Evaluation of fluoride-induced metal
584 mobilization in soil columns. Journal of environmental quality 29:454-459.
585 Tributh H, Lagaly G (1986) Aufbereitung und Identifizierung von Boden-und Lagerstättentonen.
586 II Korngrößenanalyse und Gewinnung von Tonsubfraktionen. GIT-Fachzeitschrift für
587 das Laboratorium 30:771-776.
588 Weerasooriya R, Wickramarathna H (1999) Modeling anion adsorption on kaolinite. Journal of
589 colloid and interface science 213:395-399.
590 Weerasooriya R, Wickramarathne H U S, Dharmagunawardhane H. A. (1998) Surface
591 complexation modeling of fluoride adsorption onto kaolinite. Colloids and Surfaces A:
592 Physicochemical and Engineering Aspects 144: 267–273.
593 WetterKontor (2019) Wetterrückblick Feldberg im Schwarzwald (1486 m). WetterKontor.
594 Yli-Halla M, Mokma DL, Wilding LP (2006) Formation of a cultivated Spodosol in east-central
595 Finland. Agricultural and Food Science 15:12-22.

596 Yuita K (1983) Iodine, bromine and chlorine contents in soils and plants of Japan AU. Soil
597 Science and Plant Nutrition 29:403-428. doi: 10.1080/00380768.1983.10434645.
598 Zhang C, Li Z, Gu M, Deng C, Liu M, Li L (2010) Spatial and vertical distribution and pollution
599 assessment of soil fluorine in a lead-zinc mining area in the Karst region of Guangxi,
600 China. Plant, Soil and Environment 56:282-287.

601

602 **Figures**

603 **Figure 1. (a)** Simplified overview of all soil sample locations from the Feldberg, southwest
604 Germany, including depiction of the typical forest at the investigated site. C = with canopy, OC
605 = without canopy, **(b)** Schematic vertical soil profile of the investigated Cambisol and the
606 corresponding soil horizons.

607 **Figure 2. (a)** Amount of C_{org} in % of different particle sizes and soil depth, **(b)** pH data for each
608 soil depth, pH = $CaCl_2$, **(c)** amount of coarse, medium and fine clay fractions in % (in relation
609 to bulk soil composition) for each soil depth, **(d)** content of pedogenic oxides in mg kg^{-1} for
610 each soil depth. Al_{ox}, Fe_{ox} = poorly crystalline Al and Fe oxides, Al_d and Fe_d = sum of poorly
611 crystalline and crystalline Al and Fe oxides. **(b) – (d)** data from Epp et al. (2020).

612 **Figure 3. (a)-(d)** Vertical depth patterns of total halogen concentrations (incorporated and
613 adsorbed + inorganic and organic; mg kg^{-1}) in four different soil size fractions. Dark blue =
614 bulk soil data from Epp et al. (2020), n = 18, light blue = halogen concentration in soil size
615 fraction 20-63 µm, n = 6; pink = halogen concentration in soil size fraction 2-20 µm, n = 6;
616 grey = halogen concentration in soil size fraction 0.2-<2 µm, n = 6 and green = halogen
617 concentration in soil size fraction 0.02-0.2 µm, n = 6. For the horizon thicknesses on the y axis
618 average values were taken over all profiles for each soil horizon. The error bars show the
619 standard deviation.

620 **Figure 4. (a)-(d)** four different soil size fractions coarse silt (20-63 µm), fine to medium silt (2-
621 20 µm), coarse clay (0.2-<2 µm) and medium clay (0.02-2 µm) versus adsorbed (%) halogen
622 amount in mineral topsoil (Ah) and subsoil (Bw1 and Bw2C). Grey bars illustrate the entire
623 range of halogens in percentage. Black dot marks mean values over all horizons in each particle
624 size.

625

626 **Appendix**

627 **Figure A1. (a)** and **(b)** Dissolved inorganic F and Cl concentrations in the supernatant
628 phosphate solution in each soil size fraction and each soil horizon after the desorption treatment
629 of the soil samples in mg L^{-1}. Residual solution of all soil size fractions of each soil horizon
630 were analyzed by ion chromatography.

631 **Figure A2. (a)-(d)** Adsorbed halogen concentrations of all soil size fractions versus Al_{ox}, Fe_{ox}
632 (poorly crystalline Al and Fe oxides) and vs Al_d and Fe_d (sum of poorly crystalline and
633 crystalline Al and Fe oxides).

634

635 **Tab. 1** Coordinates of sample positions.

ID	Name	Lage (Gauss-Krüger, Potsdam, R + H)		WGS84
C1	Canopy 1	3424944	5304667	N 47.875794 E 7.995611
C2	Canopy 2	3424943	5304681	N 47.875919 E 7.995595
C3	Canopy 3	3424919	5304667	N 47.875791 E 7.995276
OC1	Open Canopy 1	3424904	5304647	N 47.875609 E 7.995079
OC2	Open Canopy 2	3424923	5304628	N 47.875440 E 7.995337
OC3	Open Canopy 3	3424888	5304631	N 47.875463 E 7.994868

636

637

638

Tab. 2 Halogen concentrations in mineral topsoil and subsoil of different soil size fractions. Horizons were classified according to IUSS Working Group-WRB (2015). Total = halogen concentration adsorbed + incorporated (= inorganic + organic), inc. = halogen concentration incorporated, ads. = halogen concentration adsorbed, "-" = no further sample material available.

Horizon (each n =1)	Size fraction	Mass fraction (wt.%)	Br					Cl					F					I					C_{org} (wt.%)
			total (mg kg^{-1})	inc. (mg kg^{-1})	% inc.	ads. (mg kg^{-1})	% ads.	total (mg kg^{-1})	inc. (mg kg^{-1})	% inc.	ads. (mg kg^{-1})	% ads.	total (mg kg^{-1})	inc. (mg kg^{-1})	% inc.	ads. (mg kg^{-1})	% ads.	total (mg kg^{-1})	Inc. (mg kg^{-1})	% inc.	ads. (mg kg^{-1})	% ads.	
Ah	20-63	15	42	36	85	6	15	225	149	66	76	34	516	567	110	0	0	7	7	94	0.4	6	9.7
Bw1			36	30	85	5	15	118	102	86	16	14	579	288	50	291	50	9	4	38	6	62	4.2
Bw2C			25	26	104	0	0	115	89	78	25	22	578	630	109	0	0	7	2	30	5	70	2.6
Ah	2-20	26	38	37	97	1	3	143	124	86	20	14	611	680	111	0	0	14	5	37	9	63	8.2
Bw1			67	48	72	19	28	106	84	80	21	20	680	616	91	64	9	18	9	49	9	51	3.8
Bw2C			63	49	77	15	23	117	89	77	27	23	678	680	100	0	0	22	8	35	14	65	-
Ah	0.2- 2	3	44	37	85	7	15	175	132	76	42	24	694	648	93	46	7	17	8	48	9	52	-
Bw1			84	64	76	29	24	123	114	93	9	7	635	816	129	0	0	24	13	53	12	47	4.3
Bw2C			79	60	76	19	24	159	112	71	47	29	755	753	100	2	0	26	12	46	14	54	6.2
Ah	0.02-0.2	0.9	156	-	-	-	-	1845	-	-	-	-	487	-	-	-	-	24	-	-	-	-	-
Bw1			170	68	40	103	60	607	114	19	493	81	707	679	96	27	4	52	18	35	3	65	58
Bw2C			153	45	29	108	71	1299	142	11	1158	89	629	653	104	0	0	41	12	29	29	71	-

Figure 1

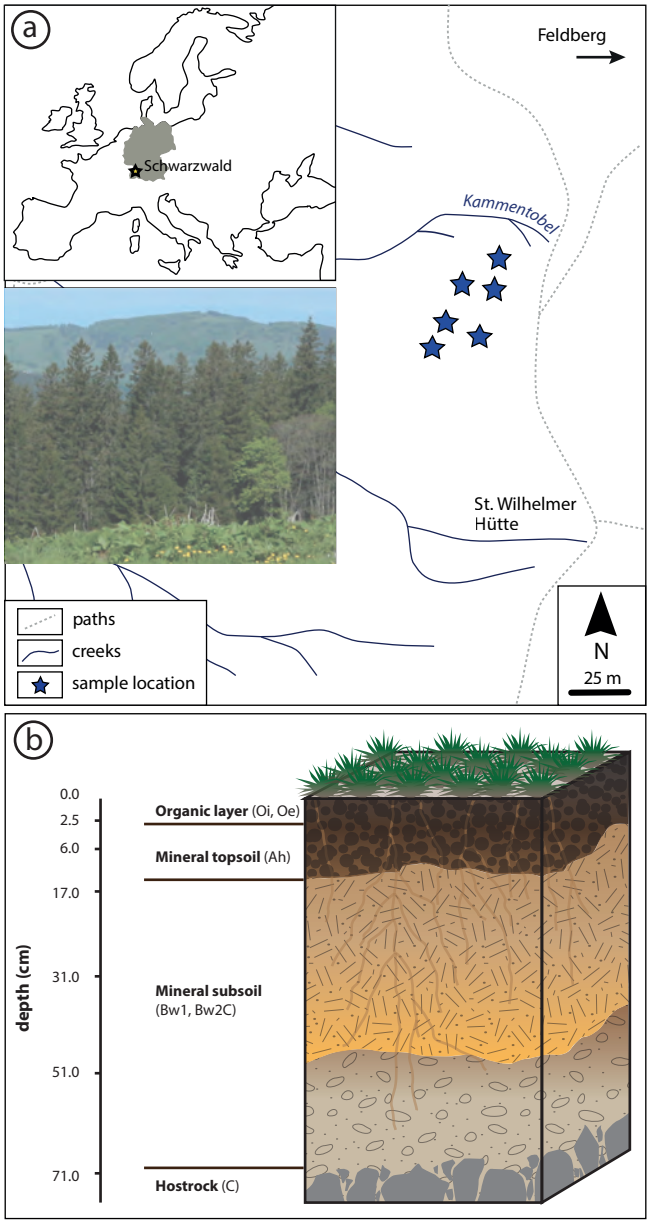
a
Schwarzwald
Feldberg
Kammentobel
St. Wilhelmer
Hütte
paths
creeks
sample location
N
25 m
b
depth (cm)
0.0
2.5
6.0
17.0
31.0
51.0
71.0
Organic layer (Oi, Oe)
Mineral topsoil (Ah)
Mineral subsoil
(Bw1, Bw2C)
Hostrock (C)

Figure 2

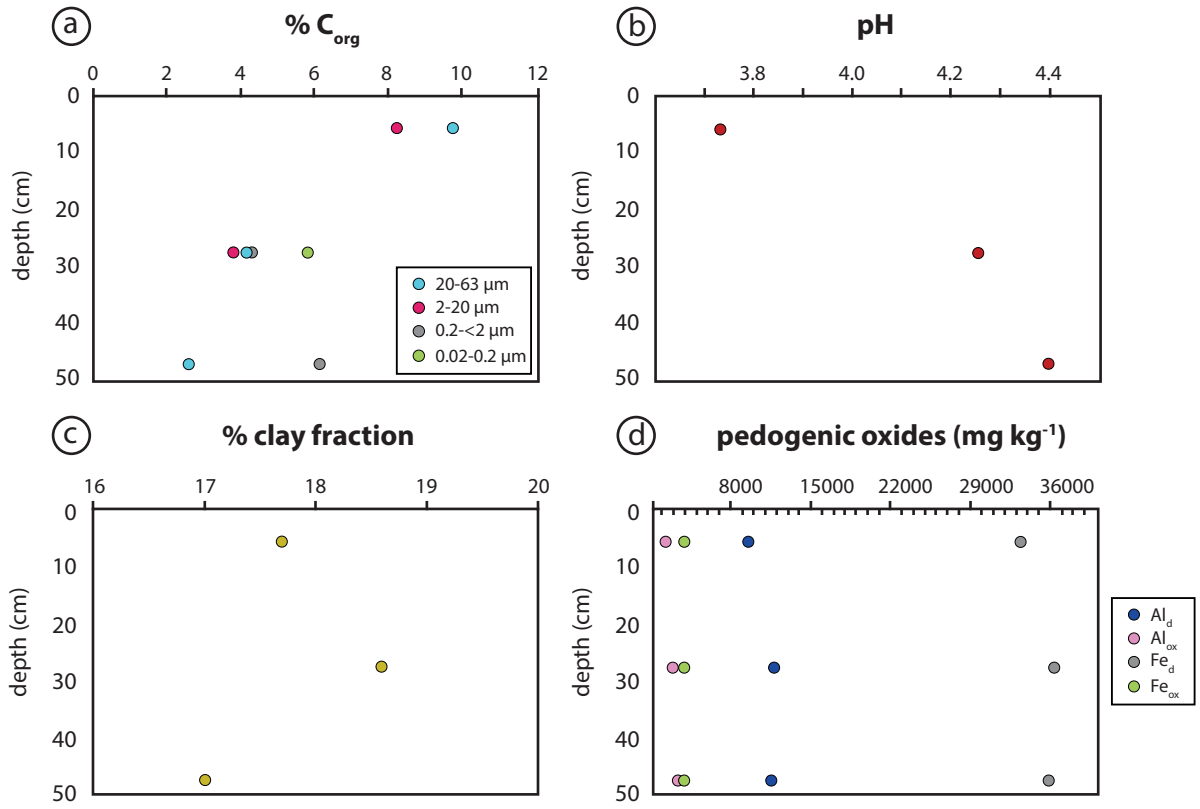
a
% C org
0
2
4
6
8
10
12
depth (cm)
0
10
20
30
40
50
20-63 µm
2-20 µm
0.2-<2 µm
0.02-0.2 µm
b
pH
3.8
4.0
4.2
4.4
c
% clay fraction
16
17
18
19
20
d
pedogenic oxides (mg kg-1)
8000
15000
22000
29000
36000
Ald
Alox
Fed
Feox

Figure 3

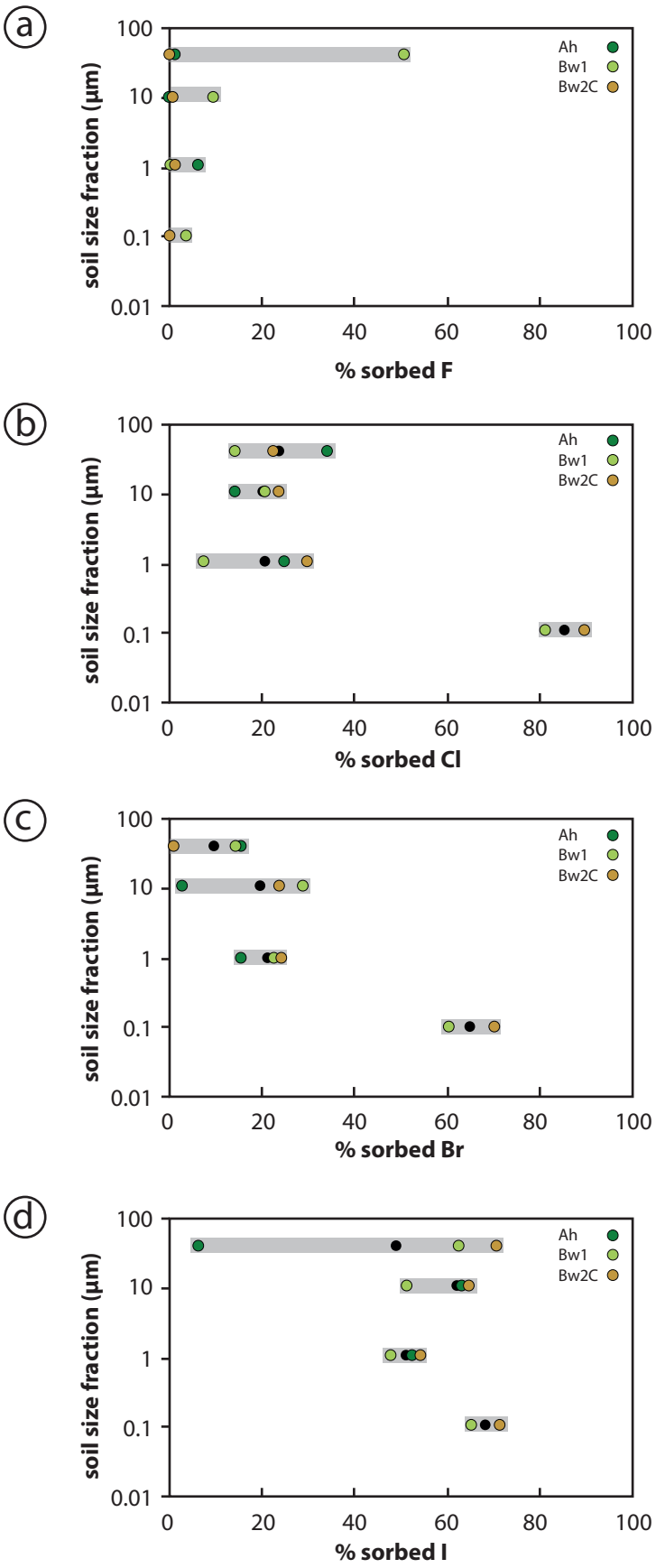
a
b
c
d
soil size fraction (µm)
100
10
1
0.1
0.01
0
20
40
60
80
100
% sorbed F
% sorbed Cl
% sorbed Br
% sorbed I
Ah
Bw1
Bw2C

Figure 4

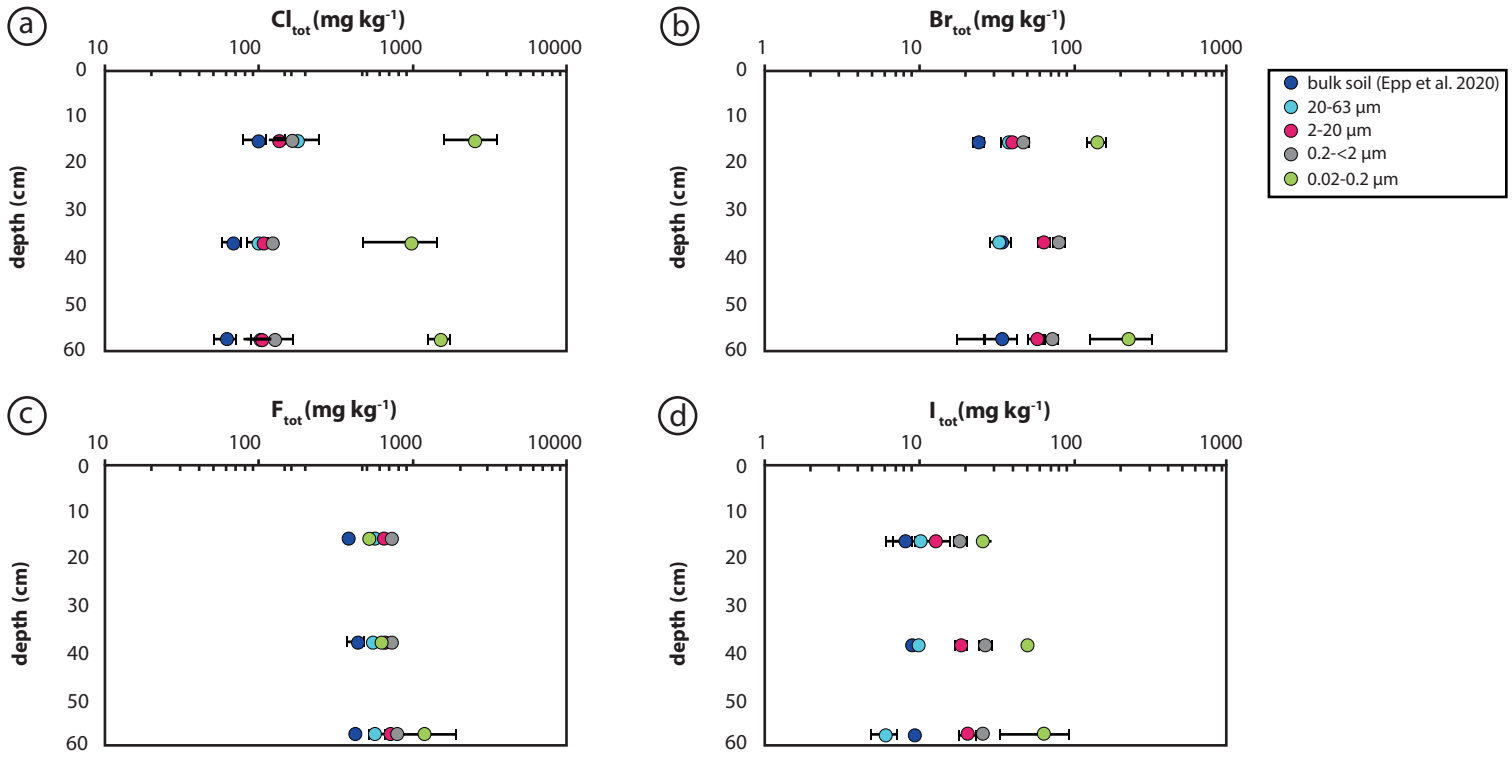
a
Cl_{tot} (mg kg^{-1})
10
100
1000
10000
depth (cm)
0
10
20
30
40
50
60
b
Br_{tot} (mg kg^{-1})
1
10
100
1000
depth (cm)
bulk soil (Epp et al. 2020)
20-63 µm
2-20 µm
0.2-<2 µm
0.02-0.2 µm
c
F_{tot} (mg kg^{-1})
10
100
1000
10000
depth (cm)
d
I_{tot} (mg kg^{-1})
1
10
100
1000
depth (cm)